

- and monitored as described (34). All manipulations (virus inoculation, physical exam, and venapuncture) were performed under ketamine sedation. To compensate for increased salivation during sedation, which would enable an accelerated flux of applied virus to the gastrointestinal tract, we injected intravenously an anti-cholinergic glycopyrroniumbromide just before virus inoculation. For atraumatic exposure of the palatine and lingual tonsils, a cotton-wool swab was saturated with phosphate-buffered saline, squeezed out, and then saturated with an undiluted or 1:10 diluted cell-free virus suspension. Thereafter, these tonsillar regions were repeatedly touched lightly in three 5-min intervals with freshly saturated swabs, finally applying a total volume of ~50 to 80 μ l of virus suspension. This applied amount of virus was calculated by weighing the swabs after use and corresponded to ~2000 to 3000 TCID₅₀ with undiluted virus (which corresponds to amounts used in many studies of urethral, rectal, and vaginal transmission) and ~200 to 300 TCID₅₀ with the diluted virus. At the time of inoculation, no obvious lesions or gingivitis were observed in the oral cavity of any of the animals used. To monitor long-term infection by this route, we followed three macaques, two receiving undiluted virus and one 1:10 diluted virus, for a longer period of time. To determine the site of virus entry and virus spread, we euthanized another eight monkeys in the acute phase after tonsillar exposure, two each on days 2, 3, and 4 and one each on days 7 and 23 after inoculation. Tonsillar infection was compared with the iv route by infecting other animals intravenously with a similar dose of 2000 TCID₅₀ of the same virus stock and monitoring them with virologic assays for several weeks and by histology in one animal on day 4. At necropsy lymphoid and nonlymphoid organs were sampled from various body locations for virus isolation, histology, immunohistochemistry, and in situ hybridization.
20. Cell-associated viral loads were determined by limiting dilution coculture with mononuclear cells from blood and lymphoid organs (35). PBMCs were separated from whole citrated blood by Ficoll density gradient centrifugation. To prepare mononuclear cells from lymphoid organs (tonsils, lymph nodes from different regions, spleen, thymus, and Peyer's patches), we forced the respective tissues through commercial nylon sieves (100- μ m mesh, Falcon) and processed them like PBMCs except for the density gradient centrifugation. This centrifugation step was only necessary for spleen cells because of the red blood cell contamination. After separation of mononuclear cells, they were simultaneously cocultivated in declining concentrations with human C81-66 T cells as indicators (35). Cultures were monitored for syncytia formation, and intracellular antigen was visualized by an immunoperoxidase assay (36), with the modification that the T cells were adhered to concanavalin A-coated microtitre plates instead of poly-L-lysine-coated plates. All treated cells were scored under a light microscope, with infected cells being identified by a deep red-brown cytoplasmic staining. The endpoint of the viral load was calculated as described (35, 37). Heat-inactivated whole SIV lysate was used in optimal concentrations to coat 96-well microtitre plates to measure serum anti-SIV antibody responses as described (36). Antigenemia was measured by a commercial HIV-1/HIV-2 antigen test (Innogenetics, Zwijndrecht, Belgium). To determine the absolute CD4⁺ T cell counts in blood, we stained PBMCs with phycoerythrin-conjugated antibody to CD4 (OKT4, Ortho Diagnostics Systems) and analyzed them on an EPICS XL flow cytometer (Coulter) with gating on lymphocytes. CD4⁺ T cell numbers were calculated by multiplying white cell count times lymphocyte percentage in a blood smear times CD4⁺ T cell percentage by fluorescence-activated cell sorting (FACS).
 21. C. Stahl-Hennig et al., data not shown.
 22. The 5- μ m-thick paraffin or cryostat sections were placed on slides coated with 3-amino-propyl-triethoxysilane. Four sections from each tissue per time point were hybridized with an ³⁵S-labeled, single-stranded, antisense RNA probe of SIVmac239 (Lofstrand Labs, Gaithersburg, MD). It was composed of fragments of 1.4 to 2.7 kb in size, which collectively represent ~90% of the SIV genome. As a positive control, cytosin preparations of SIV-infected PBMCs were hybridized, and as a negative control, a sense-strand probe was used. Dewaxed paraffin sections were boiled in a domestic pressure cooker in citrate buffer pH 6.0 for 5 min, chilled down to room temperature, rinsed in water containing 2% diethyl-pyrocabonate, and prehybridized for 2 hours at 45°C. The prehybridization mixture consisted of 50% formamide, 0.5 M NaCl, 10 mM tris-HCl at pH 7.4, 1 mM EDTA, 0.02% Ficoll-polyvinylpyrrolidone, and 2 mg of tRNA per milliliter. Prehybridization was followed by incubation with the hybridization mixture (prehybridization mixture, 10% dextran sulfate, and 2 \times 10⁶ dpm of probe per milliliter) overnight at 45°C in a moist chamber. After several washings in standard saline citrate (SSC), the sections were digested with ribonuclease at 37°C for 40 min, washed again in 2 \times SSC, dehydrated, and dipped in Kodak NTB-2 emulsion. Exposure at 4°C was for 2 to 3 days for frozen sections and 7 days for paraffin sections. After development in Kodak D-19, sections were counterstained with hemalaun, mounted, and examined with an Axiophot Zeiss microscope equipped with epiluminescent illumination. Viral RNA-positive cells were counted with a 20 \times objective, a 3CD color camera, and a PC-based image analysis system (KS400; Kontron, Esching, Germany). Positive cells had >20 silver grains, corresponding to a sixfold excess over background. Four entire sections were counted for each recorded value to obtain a mean number of infected cells per section and per unit area. The percentage of infected cells was then recorded for the epithelial, germinal center, and extrafollicular lymphoid tissue.
 23. Immunolabeling was performed on paraffin-embedded and cryostat sections according to the alkaline phosphatase anti-alkaline phosphatase method. Antibodies included CD68 (Dako, macrophages), CK1 (Dako, cytokeratin), p55 (provided by E. Langhoff, mature DCs), CD1a (Immunotech, immature DCs), CD4 (Leu3a, Becton Dickinson; OKT4, Ortho Diagnostics; and NCL, CD-4 1F6 Novocastra; all together), CD8 (Leu2a, Becton Dickinson, and C8/144B, Dako; together), and polyclonal CD3 (Dako, visualized with the peroxidase anti-peroxidase method). Immunolabeling was performed before in situ hybridization.
 24. K. Tenner-Racz et al., *AIDS* 2, 299 (1988).
 25. T. W. Baba et al., *Science* 272, 1486 (1996).
 26. R. M. Ruprecht et al., *AIDS Res. Hum. Retrovir.* 14, S97 (1998).
 27. R. B. Rothenberg, M. Scarlett, C. del Rio, D. Reznik, C. O'Daniels, *AIDS* 12, 2095 (1998).
 28. K. Tenner-Racz, P. Racz, Q. N. Myrvik, J. R. Ockers, R. Geister, *Lab. Investig.* 41, 106 (1979).
 29. B. Winther, D. J. Innes, *Arch. Otolaryngol. Head Neck Surg.* 120, 144 (1994).
 30. P. Brandtzaeg, in *Immunology of the Ear*, J. Bernstein and P. Ogra, Eds. (Raven Press, New York, 1987), p. 63.
 31. S. S. Frankel et al., *Am. J. Pathol.* 151, 89 (1997).
 32. A. Granelli-Piperno, V. Finkel, E. Delgado, R. M. Steinman, *Curr. Biol.* 9, 21 (1998).
 33. A. Granelli-Piperno et al., *J. Exp. Med.* 184, 2433 (1996).
 34. K. L. Molnar-Kimber et al., *Hum. Gene Ther.* 9, 2121 (1998).
 35. C. Stahl-Hennig et al., *J. Gen. Virol.* 77, 2969 (1996).
 36. S. G. Norley, J. Lower, R. Kurth, *Biologicals* 21, 251 (1993).
 37. C. Stahl-Hennig, et al., *Virology* 186, 588 (1992).
 38. We thank A. Aubertin (Strasbourg, France) for providing an early passage of SIVmac251. The ³⁵S-labeled, single-stranded, antisense RNA probe of SIVmac239 (Lofstrand Labs, Gaithersburg, MD) was obtained in collaboration with S. Gartner (Yale University, New Haven, CT) through the NIH Research Program. Grant support was provided by the NIH (AI 42129 and 40874 to R.M.S., and AI 40877 to M.P.), the German Ministry of Education and Research (BMBF, grant number 01KI-9767/9), the Korber Foundation (Hamburg), and the Fogarty Foundation (RO3TW00792).
- 16 February 1999; accepted 22 July 1999

Conservatism of Ecological Niches in Evolutionary Time

A. T. Peterson,¹* J. Soberón,² V. Sánchez-Cordero³

Theory predicts low niche differentiation between species over evolutionary time scales, but little empirical evidence is available. Reciprocal geographic predictions based on ecological niche models of sister taxon pairs of birds, mammals, and butterflies in southern Mexico indicate niche conservatism over several million years of independent evolution (between putative sister taxon pairs) but little conservatism at the level of families. Niche conservatism over such time scales indicates that speciation takes place in geographic, not ecological, dimensions and that ecological differences evolve later.

Critical characteristics of species' biology, such as physiology, feeding ecology, and reproductive behavior, define their fundamental ecological niches (1). In the early 1990s, several theoretical community ecologists independently predicted that fundamental niches of species under natural selection could change, but slowly. Based on diverse models

that coupled population and genetic dynamics in heterogeneous environments, niche conservatism was predicted, because rates of adaptation in environments outside of the fundamental niche would often be slower than the extinction process (2).

However, little empirical evidence has been assembled to address these theoretical predictions (3). One study (4) that compared population response surfaces to climatic conditions in two closely related species of beeches (*Fagus* spp.) showed that limiting conditions for the presence of populations were coincident. Another study (5) documented conservatism in geographic range size in disjunct Asian and North American

¹Natural History Museum, The University of Kansas, Lawrence, KS 66045, USA. ²Instituto de Ecología, Universidad Nacional Autónoma de México, México, D.F. 04510, México. ³Departamento de Zoología, Instituto de Biología, Universidad Nacional Autónoma de México, México, D.F. 04510, México.

*To whom correspondence should be addressed. E-mail: town@ukans.edu

REPORTS

plant taxa but focused principally on distributional area as opposed to ecological niche characteristics. Other recent studies, however, have revealed rapid (over about 100 years) niche evolution that may be linked to speciation (6). These two contrasting views remain to be tested in broad samples of taxa to assess the generality of niche conservatism on evolutionary time scales.

We now apply new tools and approaches to examine this question in birds, mammals, and butterflies in an arena of active speciation and population differentiation—the Isthmus of Tehuantepec in southern Mexico (7). Drawing on extensive databases that summarize scientific specimen holdings, we examined 21 sister taxon pairs of birds, 11 sister taxon pairs of mammals, and 5 sister taxon pairs of butterflies and tested the degree to which ecological characteris-

tics of one taxon were able to predict (with an artificial intelligence algorithm) the geographic distribution of its putative sister taxon and vice versa. To provide comparisons over longer time scales, we also analyzed randomly chosen confamilial, nonsister taxa (8–11).

Based on large-scale ecological dimensions, the approach uses a genetic algorithm to produce a set of decision rules in ecological space (a model of the fundamental niche) that can be projected onto maps to predict potential geographic distributions. Modeling each member of the putative sister taxon pairs in this study yielded not just a predicted geographic range approximating its own geographic distribution but also a predicted range mirroring the geographic distribution of its allopatric sister taxon. For example, for the hum-

mingbird species pair *Atthis heloisa* (north and west of the isthmus) and *Atthis ellioti* (south and east of the isthmus), the model for *A. heloisa* successfully predicted all six occurrence points available for *A. ellioti*, and the model for *A. ellioti* predicted 66 of 79 occurrence points for *A. heloisa* (Fig. 1A). Statistical significance of the *Atthis* comparisons was clear, with probabilities at about 0.03 for the first comparison and at about 10^{-22} for the second. Across the 37 pairs, 32 eastern taxa predicted distributions of western taxa significantly, and 26 western taxa predicted distributions of eastern taxa significantly (Fig. 1). When we examined significant and nonsignificant predictive models, we noted a strong relationship with sample size: models were nonsignificant only at sample sizes of <15 points for the predicted taxon (Fig. 2). For all taxon pairs, at least one of the reciprocal predictions was statistically significant. When we compared the ability of each taxon to predict its sister taxon's distribution with its ability to predict the distributions of all other taxa on the opposite side of the Isthmus of Tehuantepec, the difference was marked and statistically significant (12). In contrast, only a few predictions of distributions of confamilial taxa were statistically significant regardless of sample size (Fig. 2).

The above analyses show conservative evolution in ecological niches of 37 sister taxon pairs of birds, mammals, and butterflies isolated on either side of the lowland barrier Isthmus of Tehuantepec. The forested habi-

Fig. 1. Geographic distributions of *A. heloisa* (circles) and *A. ellioti* (squares) (A), *P. melanocarpus* (circles) and *P. zarhynchus* (squares) (B), and *P. c. charops* (circles) and *P. c. nigricans* (squares) (C). Occurrence points for each taxon are overlaid on geographic predictions based on the ecological characteristics of occurrence points of its sister taxon (dark gray for east of Isthmus of Tehuantepec predicting west, light gray for converse). Dashed lines show approximate position of the Isthmus of Tehuantepec.

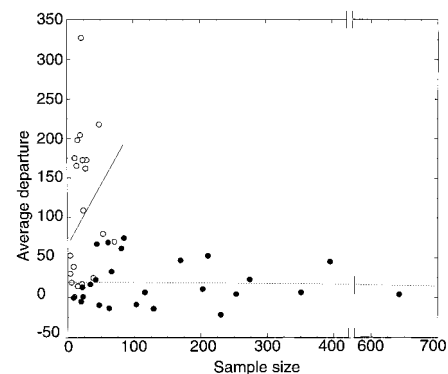
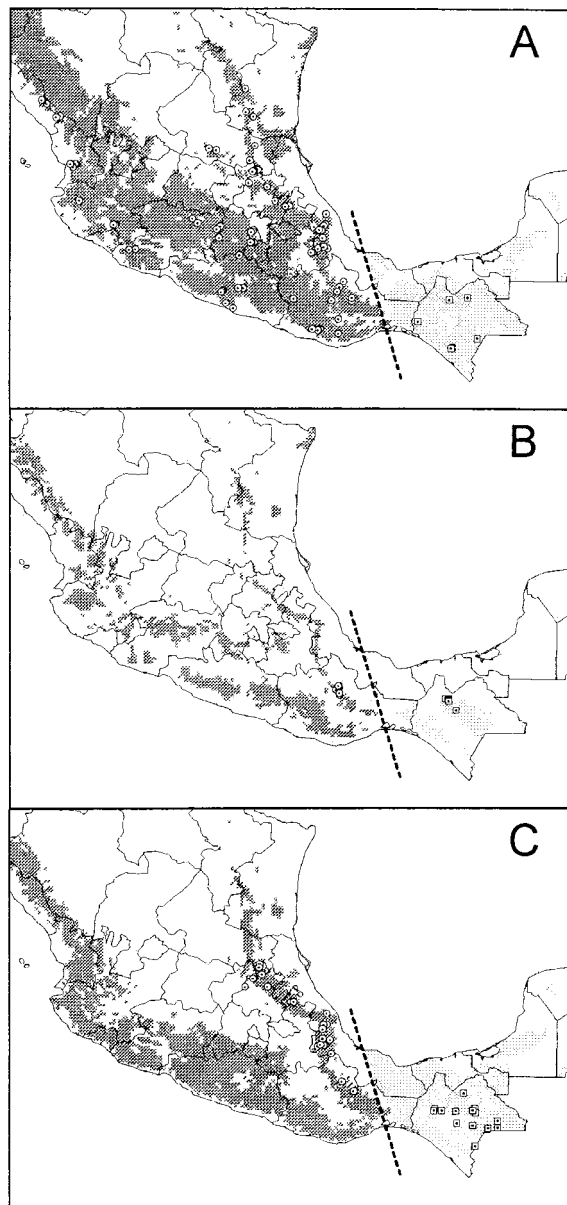


Fig. 2. Graph of average departure in reciprocal predictions among putative sister taxon pairs (open symbols) and confamilial species pairs (filled symbols), illustrating the significant interpredictiveness among sister taxa and the nonsignificant interpredictiveness among distantly related, confamilial taxa. Vertical axis represents the average of χ^2 values for interpredicting taxon pairs, taking into account direction of departure from expectation (that is, predictions worse than expectation are assigned negative values). Solid and dashed lines represent linear regressions of departure values on sample size for sister-taxon and confamilial comparisons, respectively.

tats on either side of the isthmus have been isolated for 2.4 to 10×10^6 years (13); hence, the observed conservatism has held for effectively twice that time of independent evolution in the pairs of lineages involved. Although ages of "families" are disputed (14), this expanded time scale (perhaps 10 to 50×10^6 years) has been sufficient to permit evolutionary diversification in niche characteristics. Hence, our results broadly confirm theoretical predictions of relative conservatism in ecological characteristics of species.

Conservatism of ecological niches across moderate periods of evolutionary time also reflects the modes of speciation involved. Strict vicariant speciation depends simply on geographic isolation, whereas other scenarios, such as the peripheral isolates model of speciation and many models of sympatric speciation (15), invoke invasion of novel ecological situations as part of the speciation process. The taxa and ecological dimensions treated here support the vicariant hypothesis, with ecological differences building up later, well after the speciation event. An untested question is whether the observed conservatism results from active constraint (stabilizing selection) or whether it reflects the absence of additive genetic variation in niche-related traits (16). Similarly, our analysis does not eliminate the possibility of niches of both members of species pairs responding in parallel to broad-scale environmental changes.

To the extent that our geographic scenario is representative, our results suggest that ecological niches evolve little at or around the time of the speciation event. Rather, ecological niche differences appear to accumulate later, over the time scale of familial relationships. Finding general conservatism in ecological niches opens the door to phylogenetic studies of niche evolution, comparative evaluations of conditions under which niche conservatism breaks down, construction of predictive distributional models, and numerous other applications to questions in biogeography (estimates of α and β diversity, centers of endemism), biodiversity (foci of species diversity), and conservation biology (development of conservation prioritizations).

References and Notes

1. M. L. Rosenzweig, *Evol. Ecol.* **1**, 315.
2. R. D. Holt and M. S. Gaines, *ibid.* **6**, 433 (1992); J. S. Brown and N. B. Pavlovic, *ibid.*, p. 360; A. I. Houston and J. M. McNamara, *ibid.*, p. 243; T. J. Kawecki and S. C. Stearns, *ibid.* **7**, 155 (1993).
3. H. H. Ross, *Taxon* **21**, 253 (1972); A. J. Boucot, *J. Paleontol.* **57**, 1.
4. B. Huntley, P. J. Bartlein, I. C. Prentice, *J. Biogeogr.* **16**, 551 (1989).
5. R. E. Ricklefs and R. E. Latham, *Am. Nat.* **139**, 1305 (1992).
6. M. R. Orr and T. B. Smith, *Trends Ecol. Evol.* **13**, 502 (1998).
7. T. P. Ramamoorthy et al., *Biological Diversity of Mex-*

ico: Origins and Distribution (Oxford Univ. Press, New York, 1993).

8. We obtained distributional data for the bird, mammal, and butterfly species or distinct subspecies involved from label data on specimens in the systematic collections cited in A. T. Peterson et al. [*Ibis* **140**, 288, (1998)] and J. E. Llorente-Bousquets et al. [*Papilionidae y Pieridae de México: Distribución Geográfica e Ilustración*, Universidad Nacional Autónoma de México, México (1997)] as well as the mammal collection of the University of Kansas Natural History Museum and the Colección Nacional de Mamíferos, Instituto de Biología, Universidad Nacional Autónoma de México. Species pairs were selected according to the following criteria: (1) that they constitute clear examples of sister taxa phylogenetically (for example, the only two species in a genus or the only two well-marked subspecies in a species); (2) that they are separated by the Isthmus of Tehuantepec (with the minor exception of taxon pairs with distinct migratory and resident populations); (3) that distributions of both taxa about the isthmus fairly directly; and (4) that sample sizes available are sufficient to permit testing.
9. The following species pairs and confamilial species were included. Birds: *Accipiter striatus* + *Accipiter chionogaster*, *Buteo nitidus*; *Amazilia beryllina* + *Amazilia devillei*, *Heliomaster longirostris*; *A. heloisa* + *A. ellioti*, *Hylocharis eliciae*; *Chlorostilbon canivetii* + *Chlorostilbon salvini*, *Tilmatura dupontii*; *Colaptes cafer* + *Colaptes mexicanoides*, *Melanerpes uropygialis*; *Cyanocitta coronata* + *Cyanocitta ridgwayi*, *Cyanocorax beecheii*; *Cyrtonyx montezuma* + *Cyrtonyx ocellatus*, *Colinus virginianus*; *Doricha eliza* + *Doricha*, sp. nov. (A. T. Peterson et al., unpublished data), *Campylopterus excellens*; *Empidonax occidentalis* + *Empidonax flavescens*, *Camptostoma imberbe*; *Ergaticus ruber* + *Ergaticus versicolor*, *Pipilo chlorurus*; *Eugenes fulgens* + *Eugenes viridiceps*, *Campylopterus hemileucurus*; *Falco sparverius* + *Falco tropicalis*, *Falco mexicanus*; *Icterus pustulatus* + *Icterus sclateri*, *Pheucticus melanocephalus*; *Melanotis caerulescens* + *Melanotis hypoleucum*, *Toxostoma redivivum*; *Mimus polyglottos* + *Mimus gilvus*, *Toxostoma bendirei*; *Pheucticus chrysopheplus* + *Pheucticus aurantiacus*, *Lanio aurantius*; *Picoides jardiinii* + *Picoides sanctorum*, *Picoides scalaris*; *Salpinctes obsoletus* + *Salpinctes neglectus*, *Thryothorus maculipectus*; *Sayornis nigricans* + *Sayornis acuatica*, *Mionectes oleagineus*; *Strix varia* + *Strix fulvescens*, *Glaucidium gnoma*; and *Turdus assimilis* + *Turdus leucachen*, *Turdus infuscatus*. Mammals: *Sorex oreopolus* + *Sorex sclateri*, *Megasorex gigas*; *Sorex oreopolus* + *S. stizodon*, *Sorex milleri*; *Artibeus aztecus aztecus* + *Artibeus aztecus minor*, *Chrotopterus auritus*; *Dasyprocta mexicana* + *Dasyprocta punctata* (no other confamilial species are available in Mexico); *Habromys lepturus* + *Habromys lophurus*, *Neotoma goldmani*; *Microtus oaxacensis* + *Microtus guatemalensis*, *Peromyscus polius*; *Microtus umbrinosus* + *Microtus guatemalensis*, *Peromyscus melanophrys*; *Peromyscus melanocarpus* + *Peromyscus zarhynchus*, *Tylomys nudicaudus*; *Peromyscus megalops* + *Peromyscus zarhynchus*, *Peromyscus merriami*; and *Sciurus colliiae* + *Sciurus yucatanensis*, *Ammospermophilus leucurus*. Butterflies: *Catasticta nimbece nimbece* + *Catasticta nimbece ochracea*, *Leptophobia aripa*; *Dismorphia eunoe eunoe* + *Dismorphia eunoe chamula*, *Dismorphia amphione*; *Pereute charops charops* + *Pereute charops nigricans*, *Pyrisitia proterpia*; *Pereute charops leonilae* + *Pereute charops nigricans*, *Ascia monuste*; and *Pyrrhosticta abderus abderus* + *Pyrrhosticta abderus electryon*, *Battus eracon*. Species names and taxonomic arrangements followed the American Ornithologists' Union (*Check-list of North American Birds*, American Ornithologists' Union, Washington, DC, ed. 7, 1998) and A. T. Peterson and A. G. Navarro (unpublished data) for birds, D. E. Wilson and Reeder (*Mammal Species of the World*, Smithsonian Institution Press, Washington, DC, ed. 2, 1993) for mammals, Tyler et al. (*Swallowtail Butterflies of the Americas*, Gainesville Scientific Publishers, Gainesville, FL, 1994) for Papilionidae, and I. Vargas et al. (*J. Lept. Soc.* **50**, 97, 1996) for Pieridae.

10. Locality data were georeferenced to the nearest 10^{-3} degree and reduced to unique latitude-longitude combinations for each species. The four thematic geographic coverages used (annual mean temperature, annual mean precipitation, elevation, and potential vegetation) consisted of raster grids (7×7 km pixels) available from the Comisión Nacional para el Uso y Conocimiento de la Biodiversidad (<http://www.conabio.gob/>). Geographic distributional predictions were developed based on algorithms designed to evaluate correlations between distributional occurrences and environmental characteristics (niches). The Biodiversity Species Workshop facility developed by David Stockwell (<http://biodi.sdsc.edu/>) provides an implementation of the *Genetic Algorithm for Rule-Set Prediction* [GARP; D. R. B. Stockwell and I. R. Noble, *Math. Comp. Simul.* **33**, 385, (1992); D. R. B. Stockwell and D. Peters, *Int. J. Geogr. Inf. Sci.* **13**, 143 (1999)]. GARP works in an iterative process of rule selection, evaluation, testing, and incorporation or rejection: first, a method is chosen from a set of possibilities (logistic regression, bioclimatic rules), and then it is applied to the data and a rule is developed. Predictive accuracy is then evaluated based on 1250 points resampled from the test data set and 1250 points sampled randomly from the study region as a whole. The change in predictive accuracy from one iteration to the next is used to evaluate whether a particular rule should be incorporated into the model. The algorithm runs either 1000 iterations or until convergence. Distributional predictions from GARP may often include areas not inhabited, an effect of the modeling being focused on ecological niches instead of geographic distributions; these commission errors in some cases may be reduced by inclusion of additional ecological dimensions or may require consideration of historical factors that lead to the absence of species from habitable areas.
11. A χ^2 statistic was used to evaluate statistical significance of reciprocal predictions of taxa, with expected numbers based on points for the predicted taxon that would fall within the area predicted present if distributed randomly. Reciprocal tests were conducted for each taxon pair. To evaluate relative degrees of conservatism of ecological niches of sister taxa, we compared the reciprocally predictive accuracy of sister taxon pairs with that for randomly chosen non-sister taxa within the same family. Statistical significance of these comparisons was evaluated by using ecological models for the sister taxon pair to predict the distribution of the nonsister taxon and tested by overlay of the points available for that species by using the χ^2 approach described above.
12. A median test comparing prediction of sister taxa with that for all other taxa included in the study from a particular side of the isthmus: eastern form predicting western form, $\chi^2 = 6.31$, degrees of freedom (df) = 1, $P = 0.012$; western predicting eastern, $\chi^2 = 5.10$, df = 1, $P = 0.0239$.
13. T. Wendt, *Anales Inst. Biol. UNAM* **58**, 29 (1989); A. Graham, in *Biological Diversity of Mexico: Origins and Distribution*, T. P. Ramamoorthy et al., Eds. (Oxford Univ. Press, New York, 1993), p. 109.
14. A. Cooper and D. Penny, *Science* **275**, 1109 (1997); T. Stidham, *Nature* **396**, 29 (1998).
15. D. J. Futuyma, *Evolutionary Biology* (Sinauer Associates, Sunderland, MA, ed. 3, 1997); E. Mayr, *Animal Species and Evolution* (Harvard Univ. Press, Cambridge, MA, 1963).
16. A. D. Bradshaw, *Philos. Trans. R. Soc. London Ser. B* **333**, 289 (1991).
17. Supported by the National Science Foundation, Kansas EPSCoR, Dirección General de Asuntos del Personal Académico de la Universidad Nacional Autónoma de México, Consejo Nacional de Ciencia y Tecnología, and the National Geographic Society. We thank the Comisión para el Uso y Conocimiento de la Biodiversidad for making geographic coverages available; the curators of scientific collections for providing access to species occurrence data; R. Holt and E. Wiley for discussions; and A. Navarro Sigüenza, J. Llorente Bousquets, D. R. B. Stockwell, R. M. Timm, and H. Benítez Díaz for assistance and access to data.

27 January 1999; accepted 7 July 1999